

# GroEL Can Unfold Late Intermediates Populated on the Folding Pathways of Monellin

Ashish K. Patra and Jayant B. Udgaonkar\*

National Centre for Biological Sciences, Tata Institute of Fundamental Research, Bangalore 560065, India

Received 4 March 2009;  
received in revised form  
10 April 2009;  
accepted 20 April 2009  
Available online  
23 April 2009

The modulation of the folding mechanism of the small protein single-chain monellin (MNEI) by the *Escherichia coli* chaperone GroEL has been studied. In the absence of the chaperone, the folding of monellin occurs *via* three parallel routes. When folding is initiated in the presence of a saturating concentration of GroEL, only 50–60% of monellin molecules fold completely. The remaining 40–50% of the monellin molecules remain bound to the GroEL and are released only upon addition of ATP. It is shown that the basic folding mechanism of monellin is not altered by the presence of GroEL, but that it occurs *via* only one of the three available routes when folding is initiated in the presence of saturating concentrations of GroEL. Two pathways become nonoperational because GroEL binds very tightly to early intermediates that populate these pathways in a manner that makes the GroEL-bound intermediates incompetent to fold. This accounts for the monellin molecules that remain GroEL-bound at the end of the folding reaction. The third pathway remains operational because the GroEL-bound early intermediate on this pathway is folding-competent, suggesting that this early intermediate binds to GroEL in a manner that is different from that of the binding of the early intermediates on the other two pathways. It appears, therefore, that the same protein can bind GroEL in more than one way. The modulation of the folding energy landscape of monellin by GroEL occurs because GroEL binds folding intermediates on parallel folding pathways, in different ways, and with different affinities. Moreover, when GroEL is added to refolding monellin at different times after commencement of refolding, the unfolding of two late kinetic intermediates on two of the three folding pathways can be observed. It appears that the unfolding of late folding intermediates is enabled by a thermodynamic coupling mechanism, wherein GroEL binds more tightly to an early intermediate than to a late intermediate on a folding pathway, with preferential binding energy being larger than the stability of the late intermediate. Hence, it is shown that GroEL can inadvertently and passively cause, through its ability to bind different folding intermediates differentially, the unfolding of late productive intermediates on folding pathways, and that its unfolding action is not restricted solely to misfolded or kinetically trapped intermediates.

© 2009 Elsevier Ltd. All rights reserved.

Edited by K. Kuwajima

**Keywords:** monellin; GroEL; protein binding; protein folding; folding intermediates

## Introduction

In the cell, the proper folding of a substantial fraction of proteins is assisted by a class of proteins called chaperones. Perhaps the best-characterized

molecular chaperone is the prokaryotic chaperonin GroEL, which, together with its cochaperonin cohort GroES, facilitates the folding of many proteins.<sup>1–6</sup> The roles played by such chaperones are even more crucial when the cell experiences stress, when even those proteins that can otherwise fold by themselves fold with decreased efficiency.<sup>7–9</sup> The primary role played by GroEL appears to be to associate

\*Corresponding author. E-mail address: [jayant@ncbs.res.in](mailto:jayant@ncbs.res.in).

reversibly with folding intermediates that would otherwise associate irreversibly with each other through exposed hydrophobic surfaces and, thereby, aggregate. Another role attributed to GroEL is that it facilitates the unfolding of misfolded intermediates, either in the absence or in the presence of ATP and GroES; thus, the chaperonin may play a more active annealing role in promoting folding.<sup>1,3</sup> Much is known about how the processes of substrate protein binding to GroEL, ATP and GroES binding to GroEL, and ATP hydrolysis are coupled intricately to one another, and how these processes elicit conformational changes in the structure of GroEL.<sup>3,5,10,11</sup> Understanding the role of GroEL in facilitating folding has, however, been difficult because of the transient nature of protein folding intermediates and because of the conformational heterogeneity of the bound forms.

Early observations that proteins can fold while remaining bound to GroEL suggested that multiple conformations of the same protein can bind GroEL.<sup>6,12–15</sup> In fact, GroEL appears to have evolved to become a universal chaperone that can bind to different nonnative conformations of many different proteins, irrespective of their native structures.<sup>12,16–18</sup> It can bind to many of the intermediates that accumulate on the folding pathways of proteins, including unfolded forms, early unstructured intermediates, molten globule intermediates, late structured intermediates, and native-like states.<sup>12,19–27</sup> Little is known about what determinants in the sequence and structure of the substrate protein allow it to bind GroEL,<sup>13,25,28–31</sup> and whether structure is induced in or removed from the substrate protein upon GroEL binding. Such binding can lead to acceleration<sup>14,32–35</sup> or deceleration<sup>12,17,36</sup> of folding rates and to modulation of the energy landscape of folding so that folding is channeled along only one of many available routes.<sup>17</sup> Modulation of the energy landscape of folding may also occur by confinement of the folding protein.<sup>15,34,37,38</sup>

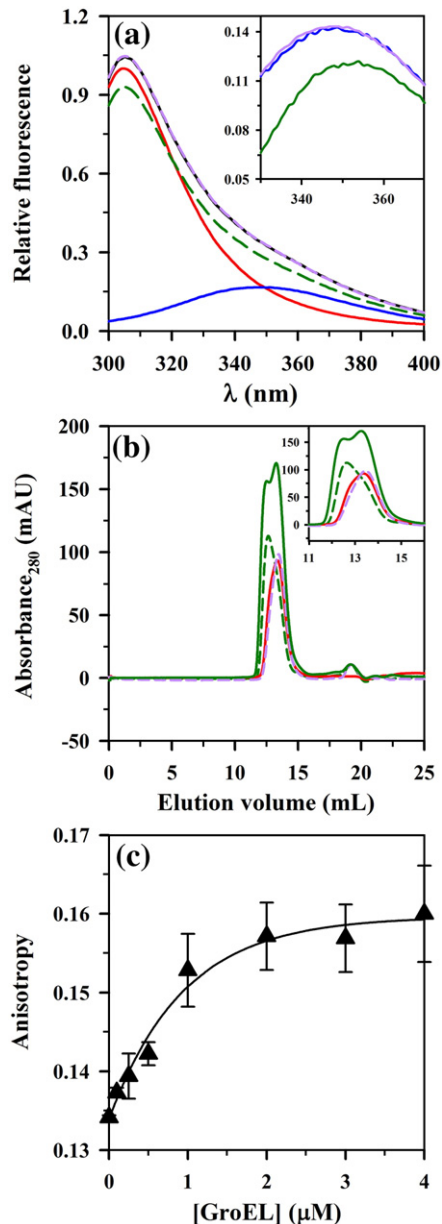


**Fig. 1.** Characterization of the interaction of GroEL with native monellin and unfolded monellin during refolding in 0.5 M GdnHCl and 0.1 M KCl (pH 7). The interaction of GroEL with unfolded monellin under refolding conditions was characterized at 2000 s after mixing an unfolded monellin solution with a refolding buffer containing GroEL in a stopped-flow mixer with a dead time of 2 ms. (a) Fluorescence spectra. Shown are the fluorescence spectra of 2  $\mu$ M monellin (blue line), 2  $\mu$ M GroEL (red line), 2  $\mu$ M GroEL mixed with 2  $\mu$ M native monellin (broken purple line), and 2  $\mu$ M GroEL mixed with 2  $\mu$ M unfolded monellin under refolding conditions (broken green line), compared to the arithmetic sum of the fluorescence spectra of 2  $\mu$ M GroEL and 2  $\mu$ M monellin (black line). Inset shows the fluorescence emission spectra of 2  $\mu$ M monellin (blue line), the mixture of 2  $\mu$ M GroEL and 2  $\mu$ M native monellin from which the GroEL fluorescence has been subtracted (purple line), and 2  $\mu$ M GroEL mixed with 2  $\mu$ M unfolded monellin under refolding conditions from which the GroEL fluorescence has been subtracted (green line). (b) Size-exclusion chromatograms. Shown are gel-filtration profiles monitored by absorbance measurements at 280 nm of 2  $\mu$ M GroEL (red line), 2  $\mu$ M GroEL mixed with 2  $\mu$ M native monellin (purple broken line), 2  $\mu$ M GroEL mixed with 2  $\mu$ M unfolded monellin under refolding conditions (green broken line), and 4  $\mu$ M GroEL mixed with 2  $\mu$ M unfolded monellin under refolding conditions (green line). Inset shows the region of the chromatogram corresponding to the elution volumes of GroEL and monellin-bound GroEL. Free monellin is seen to elute out at a volume of 18 mL for the samples prepared by mixing 2 or 4  $\mu$ M GroEL with 2  $\mu$ M unfolded monellin under refolding conditions. (c) Fluorescence anisotropy of the products of the refolding reaction of monellin carried out in the presence of different concentrations of GroEL, measured after the folding reaction has gone to completion (>2000 s). The continuous lines through the anisotropy data have been drawn by inspection. Error bars represent standard deviations from three independent measurements.

GroEL can also modulate the energy landscape of folding by unfolding partially folded intermediates, with errors in folding being removed by iterative unfolding and folding steps.<sup>39</sup> Unfolding may be achieved either through a thermodynamic coupling mechanism<sup>17,33,40,41</sup> where GroEL binds preferentially to a less structured conformation than to a more structured conformation on the folding pathway, or through a catalytic mechanism where GroEL binds to the more structured conformation.<sup>42</sup> In other models, forced unfolding of a partially folded conformation is induced by the large conformational change that GroEL undergoes upon ATP hydrolysis and subsequent GroES binding.<sup>43–45</sup> To understand the role of GroEL-enabled protein unfolding in facilitating the folding reaction, it is necessary to first demonstrate that the unfolding of folding intermediates indeed occurs during the folding of a protein whose folding mechanism has been delineated in detail. The small protein monellin appears to be a suitable model protein for such studies.

The folding mechanism of single-chain monellin (MNEI) has been characterized in detail.<sup>46–48</sup> Multiple folding pathways operate but do so at sufficiently different rates, so that individual pathways can be distinguished.<sup>47</sup> Importantly, each pathway has early collapsed intermediates, as well as later, more structured intermediates. Hence, monellin appears to be an attractive model system for the study of how GroEL might modulate the energy landscape of folding of a protein by enabling transient unfolding reactions during the course of folding. Furthermore, since monellin occurs naturally as a heterodimeric protein,<sup>49–51</sup> which, like the single-chain variant, can fold and unfold reversibly under some (but not all) conditions,<sup>52</sup> the two-chain variant would be an ideal system for studying how GroEL enables productive chain complementation within the confines of its folding chamber. Finally, since monellin is a good model system for the study of protein aggregation,<sup>53,54</sup> it could be a useful system to study how GroEL might modulate the process of protein aggregation.

In this study, it is shown that when the folding of single-chain monellin is initiated in the presence of GroEL, the chaperone modulates the folding pathways of monellin by binding differentially to different folding intermediates. The binding of GroEL is rapid, occurring at nearly a diffusion-controlled rate. While the basic folding mechanism is unperturbed by GroEL binding, the folding rates of all folding routes are modulated because of thermodynamic coupling of the binding reaction to the folding reaction. At saturating concentrations of GroEL, two of the folding routes do not appear to operate. It is shown that GroEL binds to folding intermediates on these two folding routes very tightly, in such a manner that the intermediates cannot fold further. Hence, a fraction of folding monellin molecules remains trapped in intermediate states bound to GroEL when folding of the remaining molecules is complete. These intermediate states

appear to be the initial collapsed and unstructured folding intermediates. When GroEL is added to folding monellin at different times of folding, the transient unfolding of late folding intermediates already formed on two of the folding routes can be observed.

## Results

### Native monellin does not bind to GroEL

When 2  $\mu$ M native monellin is added to 2  $\mu$ M GroEL in a buffer containing 0.5 M GdnHCl and 0.1 M KCl (pH 7), the fluorescence spectrum of the mixture is observed to be identical with the arithmetic sum of the fluorescence spectra of individual proteins (Fig. 1a). Even when the monellin concentration is in a fourfold excess over that of the GroEL concentration, the spectrum of the mixture of the two proteins is predicted by individual spectra (data not shown). No change is seen in the spectrum for incubation times as long as 48 h. Moreover, when a mixture of 2  $\mu$ M native monellin and 2  $\mu$ M GroEL in 0.5 M GdnHCl is subjected to size-exclusion chromatography, the two proteins elute out separately, and the elution profile of the GroEL in the mixture is identical with that seen with only GroEL (Fig. 1b). These results indicate that there is no interaction between the two fully folded proteins.

On the other hand, when equilibrium-unfolded monellin in 5 M GdnHCl is diluted 10-fold into a native buffer containing GroEL, using a stopped-flow machine to ensure that mixing occurs within 2 ms such that the concentrations of both proteins are finally 2  $\mu$ M in 0.5 M GdnHCl and 0.1 M KCl (pH 7), the fluorescence spectrum of the resultant mixture collected 2000 s after mixing is different from the arithmetic sum of the fluorescence spectra of 2  $\mu$ M monellin and 2  $\mu$ M GroEL (Fig. 1a), indicating that at least some of the monellin is bound to the GroEL. It should be noted that the difference from the sum is not due to the fact that some of the refolding monellin has misfolded or aggregated, since the equilibrium-unfolded protein refolds completely in the absence of GroEL.<sup>47</sup> When the fluorescence spectrum of 2  $\mu$ M free GroEL is subtracted from that of monellin-bound GroEL (Fig. 1a, inset), the resultant difference spectrum is different from that of native monellin. The wavelengths of maximum fluorescence emission by native monellin and unfolded monellin are 348 and 355 nm, respectively, while that by the GroEL-bound monellin is 352 nm, suggesting that the latter is at least partially unfolded.

Size-exclusion chromatography shows that when unfolded monellin is added to GroEL under refolding conditions using a stopped-flow machine to ensure that mixing occurs within 2 ms, some of the monellin is ultimately found free in solution after all folding reactions have been completed, even when the GroEL is present in twofold excess (Fig. 1b). The

elution profile of the protein that was allowed to refold completely in the absence of GroEL was identical with that of native monellin and showed no evidence of misfolded or aggregated protein (data not shown). A large fraction of the monellin remains bound to the GroEL, and the monellin-bound GroEL is observed to elute earlier than does free GroEL (Fig. 1b). Not surprisingly, the monellin-bound GroEL displays a higher absorbance at 280 nm, as manifested by the larger area under the chromatography peak, than does GroEL in a mixture with native monellin because of the contribution of the bound monellin on the former case.

To confirm that a fraction of refolding monellin molecules remains bound to GroEL, in whose presence refolding was initiated, the fluorescence anisotropy of the product of the folding reaction (after stopped-flow mixing) was examined after

2000 s. Figure 1c shows that the fluorescence anisotropy of the folding product increases with the concentration of GroEL in which folding was initiated. Fluorescence anisotropy increases in value from  $0.134 \pm 0.002$  for the product of folding initiated in the absence of GroEL to  $0.16 \pm 0.006$  for the product of folding initiated in the presence of 2–4  $\mu\text{M}$  GroEL (Fig. 1c). The observation that fluorescence anisotropy has reached a saturating value upon addition of 2  $\mu\text{M}$  GroEL suggests that the binding of monellin is very tight and, hence, further addition of GroEL does not lead to an increase in fluorescence anisotropy.

The value of the fluorescence anisotropy of native monellin alone ( $0.134 \pm 0.002$ ) is similar to that reported earlier for double-chain monellin.<sup>55</sup> When native monellin was mixed with GroEL, the fluorescence anisotropy value remained at 0.132,

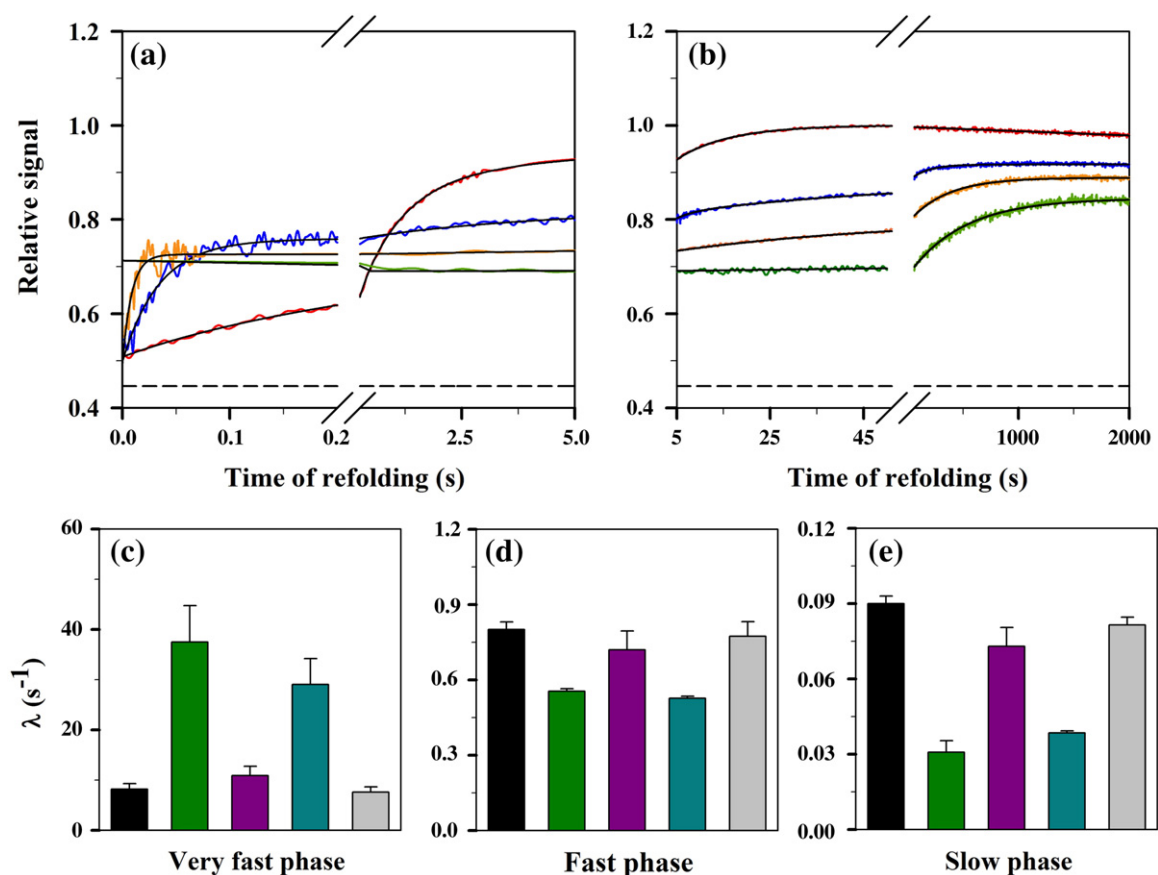


**Fig. 2.** Effect of GroEL on the refolding kinetics of monellin in 0.5 M GdnHCl and 0.1 M KCl (pH 7). Monellin (2  $\mu\text{M}$ ) was refolded in the presence of 0  $\mu\text{M}$  (red line), 0.4  $\mu\text{M}$  (blue line), 1  $\mu\text{M}$  (orange line), and 4  $\mu\text{M}$  (green line) GroEL. Refolding was determined by monitoring the fluorescence emission at 340 nm, upon excitation at 280 nm. The fluorescence of the relevant concentration of GroEL has been subtracted from each trace, and all fluorescence values were then normalized to a value of 1 for the fluorescence of monellin at 2000 s of refolding in the absence of GroEL. The black continuous lines through the data represent least-squares fits. The broken line represents the fluorescence of unfolded monellin in 5 M GdnHCl. (a) Only the first 5 s of the folding reaction are shown to illustrate the effect of GroEL on the burst, very fast, and fast phases of the folding of monellin. (b) From 5 to 2000 s of the folding reaction are shown to illustrate the effect of GroEL on the very slow phase. (c–e) The apparent rate constants of the very fast, fast, and slow phases of the folding of 2  $\mu\text{M}$  monellin in the absence of GroEL (black bar), in the presence of 0.5  $\mu\text{M}$  GroEL (green bar), in the presence of 0.5  $\mu\text{M}$  GroEL presaturated with 1 mM ATP and 2 mM  $\text{MgCl}_2$  (purple bar), in the presence of 0.5  $\mu\text{M}$  GroEL presaturated with 1 mM ADP and 2 mM  $\text{MgCl}_2$  (dark cyan bar), and in the presence of 0.5  $\mu\text{M}$  bovine serum albumin (gray bar). Error bars represent standard deviations from three separate measurements.

confirming the absence of any interaction between native monellin and native GroEL.

### Folding of monellin in the presence of GroEL

Figure 2a and b show the kinetic traces of the folding of 2  $\mu\text{M}$  monellin in the absence and in the presence of three different concentrations of GroEL. Previous studies have shown that in the absence of GroEL, the fluorescence change accompanying folding in 0.5 M GdnHCl, but in the absence of any added KCl, occurs in three phases: a very fast phase (15%) with an apparent rate constant of  $7\text{ s}^{-1}$ , a fast phase (60%) with an apparent rate constant of  $1\text{ s}^{-1}$ , and a slow phase (25%) with an apparent rate constant of  $0.1\text{ s}^{-1}$ . These kinetic phases lead to the formation of long-lived intermediates that transform into native protein in a very slow phase ( $0.0024\text{ s}^{-1}$ ), which is silent to fluorescence change. In the present study, folding was carried out in 0.5 M GdnHCl in the presence of 0.1 M KCl. KCl was added because it was necessary to maintain the stability of GroEL. The presence of 0.1 M KCl introduces an  $\sim 10\%$  unobservable burst-phase change in fluorescence at the expense of the fast and slow kinetic phases whose amplitudes reduce to 55% and 20%, respectively. The apparent rate constants are not perturbed.

Figure 2a and b shows that as the GroEL concentration is increased to 4  $\mu\text{M}$ , the following are observed: (1) a decrease in the total amplitude of the observable fluorescence change; (2) an increase in both the apparent rate constant and the relative amplitude of the very fast kinetic phase; (3) a decrease in both the apparent rate constant and the relative amplitude of the fast kinetic phase; (4) a decrease in both the apparent rate constant and the relative amplitude of the slow kinetic phase; and (5) the appearance of a very slow phase of fluorescence change, whose apparent rate does not change but whose relative amplitude shows an increase. At a GroEL concentration of 4  $\mu\text{M}$ , the very fast phase seems to disappear, as do the fast and slow phases of fluorescence change; only a burst-phase increase and a very slow increase in fluorescence are seen.

If the folding reaction is carried out in the presence of GroEL that has been presaturated with 1 mM ATP, no effect is seen on either the apparent rate constant (Fig. 2c–e) or the relative amplitude (data not shown) of either the very fast, the fast, or the slow phase of refolding. Moreover, no fluorescence change is observed to occur during the very slow phase of refolding. The effect of GroEL presaturated with ADP is the same as that of GroEL alone. If the folding reaction is carried out in the presence of bovine serum albumin instead of GroEL, again no effect is seen on the apparent rate constants and relative amplitudes of any of the kinetic phases of refolding.

### Extent of monellin folding in the presence of GroEL

The data in Figs. 1a, 2a and b, and 3a indicate that the total change in fluorescence during the folding of

monellin in the presence of GroEL is less than that seen in its absence. Figure 3a shows how the total amplitude of fluorescence change decreases with an

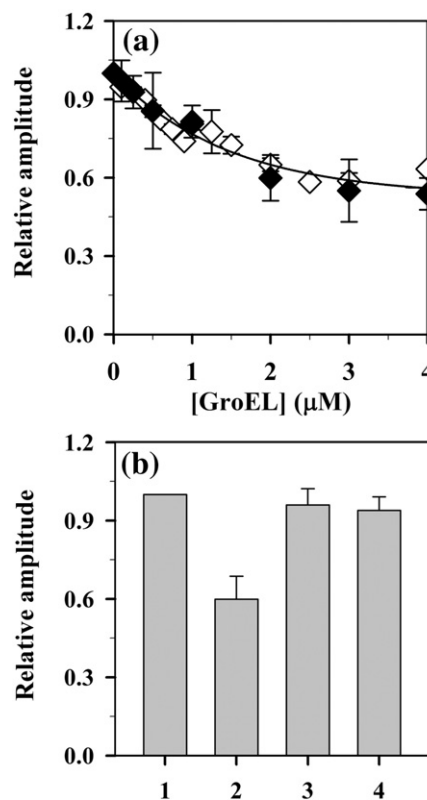


**Fig. 3.** Dependence on GroEL concentration of the total amplitude of fluorescence change during the folding reaction of monellin in 0.5 M GdnHCl and 0.1 M KCl (pH 7). (a) The relative total amplitude ( $\diamond$ ) at each GroEL concentration was determined as  $(F_G - F_U)/(F_N - F_U)$ , where  $F_U$  is the fluorescence of unfolded monellin in 0.5 M GdnHCl obtained from a linear extrapolation of the unfolded protein baseline of an equilibrium GdnHCl-induced unfolding curve determined in 0.1 M KCl (pH 7);  $F_G$  is the fluorescence of the refolded monellin at 2000 s of refolding in the presence of GroEL; and  $F_N$  is the fluorescence of refolded monellin at 2000 s of refolding in the absence of GroEL. The fluorescence of the relevant concentration of GroEL was subtracted prior to the calculation of total amplitude at each GroEL concentration. Also shown is the relative amount of free monellin ( $\blacklozenge$ ) present in solution (not bound to GroEL) after the folding reaction has gone to completion ( $>2000\text{ s}$ ). The relative amount of free monellin was determined as described in the text. (b) Bar chart showing the relative amount of free native monellin after folding has been completed at 2000 s when 2  $\mu\text{M}$  monellin is folded in the absence of GroEL (1); in the presence of 2  $\mu\text{M}$  GroEL (2); in the presence of 2  $\mu\text{M}$  GroEL, 1 mM ATP, and 2 mM  $\text{MgCl}_2$  (3); and in the presence of 2  $\mu\text{M}$  GroEL alone, but after subsequent treatment with 1 mM ATP and 2 mM  $\text{MgCl}_2$  for 2000 s (4). The relative amount of free monellin was determined from the relative fluorescence of the filtrate that passes through a 100-kDa ultrafiltration membrane after the excess of ATP had been removed by a High-trap desalting column. In all panels, error bars represent standard deviations from three separate experiments.

increase in GroEL concentration. At a GroEL concentration of 2  $\mu\text{M}$ , the observed fluorescence change is about 50–60% of that expected if the monellin were to fold completely and not be bound to the GroEL. To determine whether the observed 50–

60% increase in fluorescence is due to 50–60% of the monellin molecules having folded completely, with the remaining 40–50% remaining bound to GroEL, the product of the folding reaction (after stopped-flow mixing) was examined after 2000 s when folding

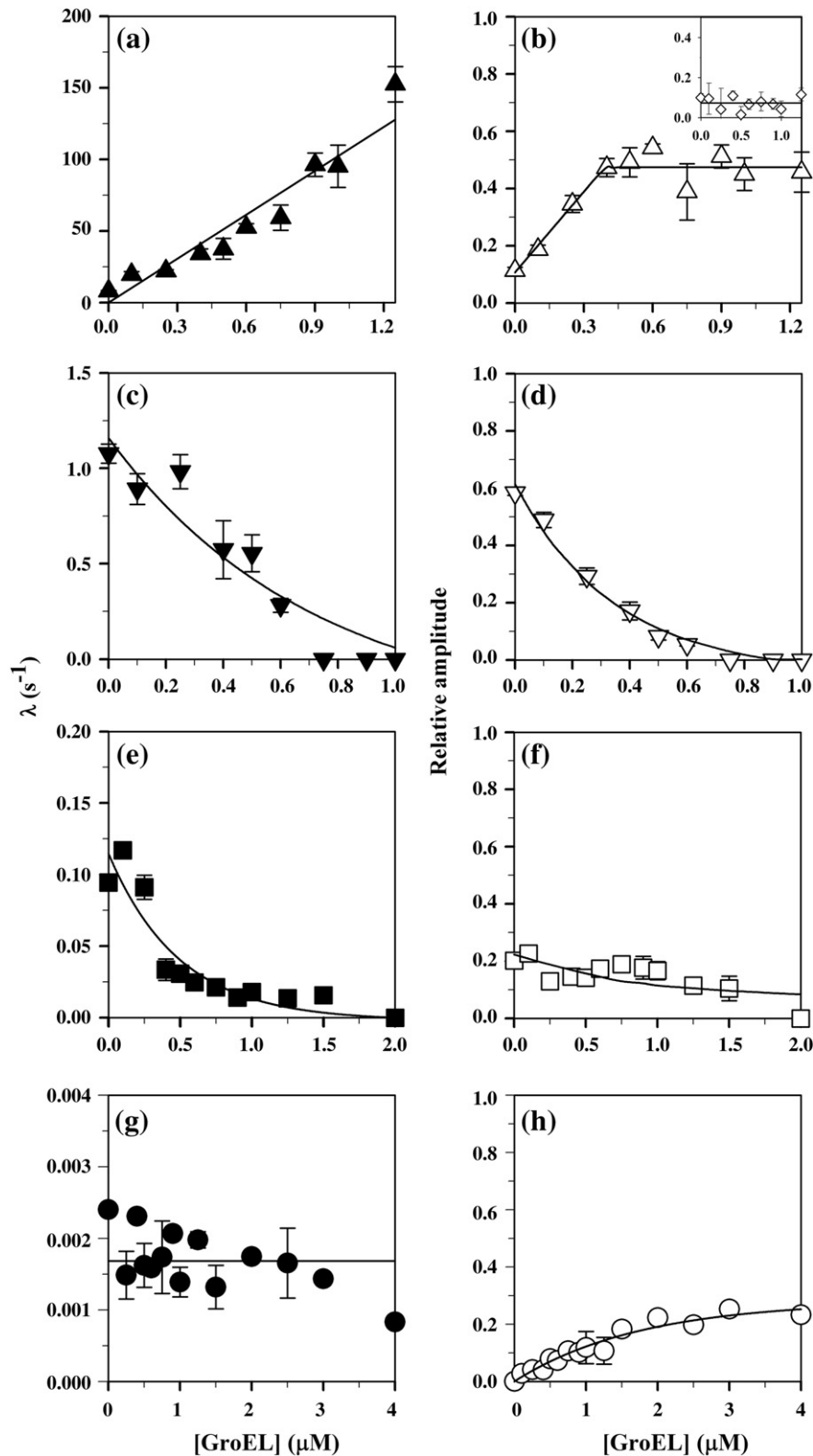


Fig. 4 (legend on next page)

had been completed. The product was filtered through a 100-kDa cutoff membrane, which allows >97% of free monellin, but <1% of GroEL, to pass through (data not shown). By measuring the fluorescence of the monellin that flowed through the membrane, the extent of free monellin and the extent of GroEL-bound monellin at the end of the folding reaction could be determined. Figure 3a shows that the relative amount of monellin that is free in solution matches the total fractional change in fluorescence during the folding of monellin at each GroEL concentration. Thus, it appears that the fractional change in fluorescence during folding in the presence of GroEL represents the fraction of monellin molecules that have folded completely and, hence, are no longer bound to GroEL. The remaining fraction of monellin molecules remains bound to the GroEL in a state whose fluorescence appears to be similar, within experimental error, to that of unfolded monellin. While the gel-filtration experiments shown in Fig. 1b indicate the same result, it has not been possible to quantify the relative amount of monellin that was free in solution because of the low absorbance at 280 nm of monellin.

Figure 3b shows that when 1 mM ATP and 2 mM MgCl<sub>2</sub> were added to the reaction mixture after the folding reaction had been allowed to proceed for 2000 s and the amount of free monellin had been determined by ultrafiltration assay, as described above, more than 95% of the monellin was found to be free in solution. Thus, the addition of ATP results in the release of the bound monellin, which subsequently folds completely while free in solution.

### Modulation of the folding kinetics of monellin by GroEL

Figure 4 shows the dependences of the apparent rate constants and relative amplitudes of the very fast, fast, slow, and very slow kinetic phases of folding on GroEL concentration.

The apparent rate constant of the very fast phase of fluorescence change appears to increase linearly with an increase in GroEL concentration from 0 to 1.25 μM (Fig. 1a). The relative amplitude increases at low GroEL concentration, but saturates abruptly at a

value of 0.5 μM. Both the apparent rate constant and the relative amplitude of the fast phase decrease with an increase in GroEL concentration of up to 0.6 μM, beyond which the fast phase cannot be observed (Fig. 4c and d). The apparent rate constant of the slow phase also decreases in value with an increase in GroEL concentration to 0.6 μM, after which it remains constant at a value of about 0.015 s<sup>-1</sup> (Fig. 4e and f). The relative amplitude remains constant within error at ~20%, even at 1.5 μM GroEL. By 2 μM GroEL, neither the very fast, fast, nor slow phase of folding can be observed.

The inset in Fig. 4b shows that the ~10% burst-phase change in fluorescence, which occurs during the first 2 ms of refolding, is unaffected by the presence of GroEL at concentrations of up to 1.25 μM GroEL. At higher GroEL concentrations, however, the burst-phase amplitude is nearly 40% (data not shown). This increase appears to occur because the very fast phase, whose rate constant increases with GroEL concentration (Fig. 2a), becomes too fast to be measured given the 2-ms dead time of mixing. Consequently, the 30% amplitude of the very fast phase gets added to the 10% burst phase seen at low GroEL concentrations.

In the presence of GroEL, unlike in its absence, a very slow phase of change in fluorescence is observed to accompany refolding. The observed fluorescence-monitored rate of 0.002 s<sup>-1</sup> is the same as the rate of the very slow phase measured previously by an interrupted folding experiment that directly measured the rate of formation of native protein,<sup>47</sup> and it appears to be independent of the GroEL concentration present (Fig. 4g). The relative amplitude of the very slow phase increases, however, with an increase in GroEL concentration up to 2 μM, after which it remains constant at about 25% (Fig. 4h).

### Effect of the delayed addition of GroEL to 1refolding monellin

When 2 μM GroEL is added at different times after the commencement of folding of 2 μM monellin, there is an initial jump in fluorescence within a few milliseconds (Fig. 5a). Subsequently, fluorescence decreases in two kinetic phases. The fast phase of

**Fig. 4.** Dependence on GroEL concentration of the kinetics of refolding of monellin in 0.5 M GdnHCl and 0.1 M KCl (pH 7). (a) Apparent rate constant of the very fast phase; (b) reduced amplitude of the very fast phase; (c) apparent rate constant of the fast phase; (d) reduced amplitude of the fast phase; (e) apparent rate constant of the slow phase; (f) reduced amplitude of the slow phase; (g) apparent rate constant of the very slow phase; and (h) reduced amplitude of the very slow phase. The reduced amplitude of each kinetic phase is equal to  $(\Delta F_i)/(F_N - F_U)$ , where  $\Delta F_i$  is the fluorescence change during the  $i$ th kinetic phase;  $F_U$  is the fluorescence of unfolded monellin in 0.5 M GdnHCl obtained from a linear extrapolation of the unfolded protein baseline of an equilibrium GdnHCl-induced unfolding curve determined in 0.1 M KCl (pH 7); and  $F_N$  is the fluorescence of refolded monellin at 2000 s of refolding in the absence of GroEL. The fluorescence of the relevant concentration of GroEL was subtracted prior to the calculation of the reduced amplitudes. The inset in (b) shows the reduced amplitude of the burst phase. The reduced burst-phase amplitude was determined as  $(F_0 - F_U)/(F_N - F_U)$ , where  $F_0$  is the fluorescence value obtained by extrapolation of the kinetic refolding curve to  $t = 0$  after subtraction of the fluorescence of the relevant concentration of GroEL. Error bars represent standard deviations from three separate experiments. The continuous line in (a) is a fit to a straight line and yields a value for  $k_b$  ( $10^8 \text{ M}^{-1} \text{ s}^{-1}$ ), the bimolecular rate constant for the association of monellin with GroEL. The continuous lines through the apparent rate constant data in (c), (e), and (g) and those through the relative amplitude data in (b), (d), (f), and (h) have been drawn by inspection.

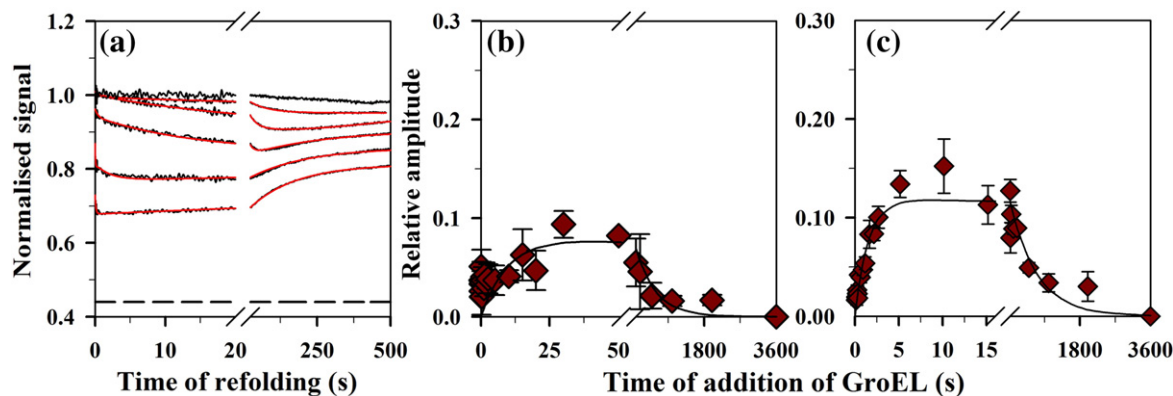


**Fig. 5.** (a) Effect of the delayed addition of GroEL on the kinetics of refolding of monellin. Monellin (2  $\mu\text{M}$ ) was refolded in 0.5 M GdnHCl and 0.1 M KCl (pH 7) for varying periods of time before the addition of GroEL in the refolding buffer to the same final concentration. (a) Kinetic traces observed subsequent to the addition of GroEL. GroEL was added at (bottom to top) 0.075, 0.5, 5, 50, 500, and 2000 s of refolding. Data are shown in black, and fits to a three-exponential equation are shown in red. No fit is shown for the 2000-s data. (b) Dependence on the time of refolding of the reduced amplitude of the fast unfolding phase seen upon addition of GroEL. The continuous line is a fit to a two-exponential equation: the amplitude increases at a rate of  $0.1 \text{ s}^{-1}$ , and then decreases at a rate of  $0.002 \text{ s}^{-1}$ . (c) Dependence on the time of refolding of the reduced amplitude of the slow unfolding phase seen upon addition of GroEL. The continuous line is a fit to a two-exponential equation: the amplitude increases at a rate of  $1 \text{ s}^{-1}$ , and then decreases at a rate of  $0.002 \text{ s}^{-1}$ . The reduced amplitudes of the fast and slow unfolding phases were determined as  $(\Delta F)/(F_N - F_U)$ , where  $\Delta F$  is the fluorescence change during the fast or slow kinetic unfolding phase;  $F_U$  is the fluorescence of unfolded monellin in 0.5 M GdnHCl obtained from a linear extrapolation of the unfolded protein baseline of an equilibrium GdnHCl-induced unfolding curve determined in 0.1 M KCl (pH 7); and  $F_N$  is the fluorescence of refolded monellin at 2000 s of refolding in the absence of GroEL. All fluorescence values in (a), (b), and (c) have been normalized to a value of 1 for the native protein in 0.5 M GdnHCl and 0.1 M KCl (pH 7) after subtraction of the fluorescence of 2  $\mu\text{M}$  GroEL.

fluorescence decrease occurs with a rate constant of  $5 \pm 2 \text{ s}^{-1}$ , while the slow phase of fluorescence decrease occurs with a rate constant of  $0.2 \pm 0.04 \text{ s}^{-1}$ . Finally, a slow increase in fluorescence, which occurs with a rate constant of  $0.002 \pm 0.0002 \text{ s}^{-1}$ , is observed. The final phase of fluorescence increase is observed only when GroEL is added within 5 s of the commencement of monellin folding.

Figure 5b and c show how the relative amplitudes of the fast and slow phases of fluorescence decrease change with the delay in adding GroEL. The relative amplitudes of both phases first increase and then decrease with an increase in the delay in adding GroEL. The rate constant of the increase in the relative amplitude of the fast phase of fluorescence decrease matches the rate constant of the increase in the population of intermediate  $I_S$ .<sup>47</sup> Similarly, the rate constant of the increase in the relative amplitude of the slow unfolding phase matches the rate constant of the increase in the population of intermediate  $I_F$ .<sup>47</sup> The rate constant of the decrease in the relative amplitude of either phase matches the rate constant for the formation of native protein from  $I_S$  or  $I_F$ . Hence, it appears that, at each time of addition of GroEL, the relative amplitude observed for each phase of fluorescence decrease represents the relative amount of the folding intermediate unfolded by GroEL. Each phase of fluorescence decrease seen in Fig. 5a therefore corresponds to an unfolding phase. Figure 5b shows that the relative amplitude of the fast unfolding phase seen upon delayed addition of GroEL first increases with a rate constant of  $0.1 \text{ s}^{-1}$ , which is the rate constant of the

formation of  $I_S$ , and then decreases with a rate constant of  $0.002 \text{ s}^{-1}$ , which is the rate constant of the formation of native monellin from  $I_S$ . The relative amplitude of the slow unfolding phase increases with a rate constant of  $1 \text{ s}^{-1}$ , which is the rate constant of the formation of  $I_F$ , and then decreases with a rate constant of  $0.002 \text{ s}^{-1}$ , which is the rate constant of the formation of native monellin from  $I_F$  (Fig. 5c).

## Discussion

### The folding mechanism of single-chain monellin is not altered in the presence of GroEL

Single-chain monellin has a complex folding mechanism: there are three principal folding routes. On one route, a very-fast-forming intermediate ( $I_{VF}$ ) is populated; on another route, two fast-forming intermediates ( $I_{F1}$  and  $I_{F2}$ ) are populated; on the third route, a slow-forming intermediate ( $I_S$ ) is populated. Each of these intermediates fold to a native protein at the same very slow rate of  $0.002 \text{ s}^{-1}$  in processes that are silent to fluorescence change, as shown in the scheme depicted in Fig. 6a. Also shown are the relative fluorescence values for the different states describing the mechanism, as deduced from experimental data.<sup>47</sup>

The scheme depicted in Fig. 6a also shows that the initial step in folding leads to a heterogeneous collapsed form,  $I_E$ .  $I_E$  consists of  $I_{E1}$ , which folds fast to  $I_F$  ( $I_{F1}$  and  $I_{F2}$ );  $I_{E2}$ , which folds slowly to  $I_S$ ; and



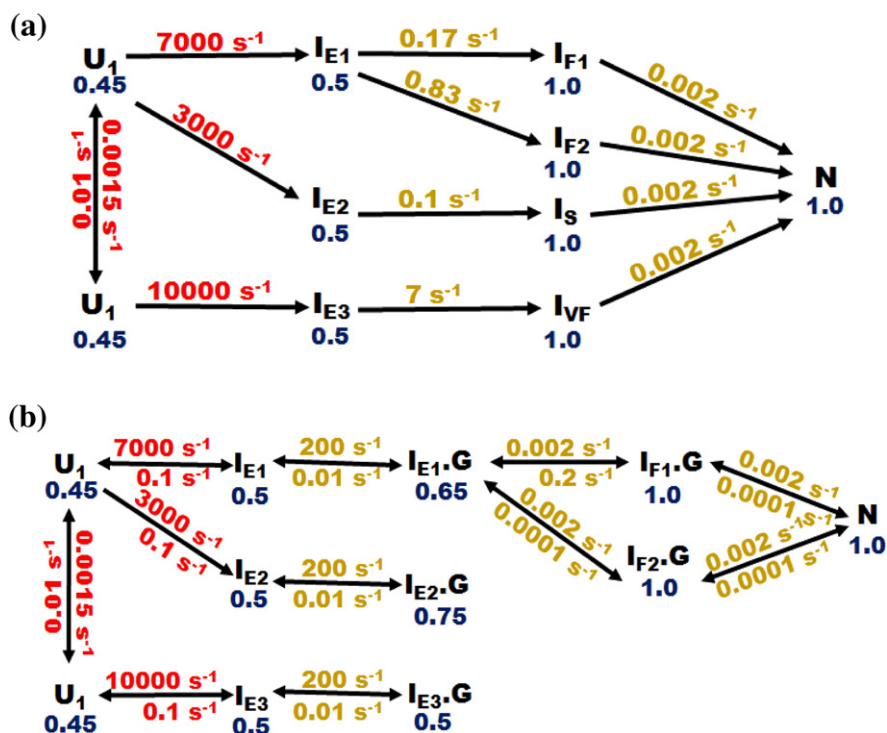


**Fig. 6.** Folding mechanisms of monellin in the absence (a) and in the presence (b) of GroEL. The scheme in (a) represents the mechanism of refolding of 2  $\mu\text{M}$  monellin in 0.5 M GdnHCl and 0.1 M KCl (pH 7) in the absence of GroEL. The scheme in (b) represents the mechanism of refolding of 2  $\mu\text{M}$  monellin in 0.5 M GdnHCl and 0.1 M KCl (pH 7) in the presence of 2  $\mu\text{M}$  GroEL. The numbers in blue are the fluorescence values of the different folding intermediates. The numbers in red (estimated) and yellow (determined from experiments) are the values of the rate constants used in kinetic simulations.

I<sub>E3</sub>, which folds very fast to I<sub>VF</sub>. The fluorescence of I<sub>E</sub> is similar to that of a completely unfolded protein; hence, U-to-I<sub>E</sub> reactions are silent to fluorescence change.

When the folding of monellin is initiated in the presence of GroEL, the very fast, fast, slow, and very slow phases of folding persist, although their apparent rate constants and relative amplitudes change with increasing GroEL concentration. A notable effect of GroEL is that the very slow folding phase is no longer silent to fluorescence change, but its apparent rate constant is not perturbed. Hence, it appears that the basic folding mechanism of single-chain monellin is not altered significantly by the presence of GroEL.

#### GroEL binds to folding intermediates but not to native monellin

When the refolding of monellin was initiated in the presence of saturating concentrations of GroEL, it was found that only about 50–60% of monellin molecules had folded completely and were present free in solution (Fig. 3). The remaining ~40–50% of the monellin molecules were found to have bound to GroEL and to remain bound even when refolding of the other 50–60% of the molecules had been completed. An analysis of the Trp fluorescence of the GroEL-bound monellin indicates that it is bound in a state whose fluorescence intensity is similar to, or marginally higher than, that of unfolded monellin

(Fig. 3a). Hence, the monellin molecules that remain tightly bound to GroEL appear either to be unfolded or to be in one or all of the collapsed intermediates (I<sub>E</sub>) that form within a few milliseconds of the commencement of refolding and whose Trp fluorescence is similar to that of unfolded monellin.<sup>47</sup> The observation that the bound monellin is released upon addition of ATP, which is known to induce conformational changes within the GroEL folding chamber<sup>56,57</sup> and thereby to reduce affinity for binding, suggests that the monellin is bound at the specific substrate-binding site of GroEL.

If 40–50% of monellin molecules remain bound to GroEL while the remaining 50–60% refold completely, it must mean that these 40–50% of molecules bind to the GroEL very tightly in such a manner that they cannot continue refolding. The very tight binding of the 40–50% of molecules to GroEL is indicated by chromatography data (Fig. 1b), fluorescence anisotropy data (Fig. 1c), and particularly by the observed dependence on GroEL concentration of the relative amplitudes of the very fast and fast phases of fluorescence change (Fig. 4b) (see Results and the text below).

The observation that native monellin does not bind to GroEL, even though partially folded forms do so, is not unusual. Human and *Escherichia coli* DHFR,<sup>25,58</sup> as well as barstar<sup>33</sup> and thioredoxin,<sup>17</sup> also do not bind GroEL; only their folding intermediates do. Neither unfolding of monellin nor its binding to GroEL can be detected even

when the two proteins are incubated together for 48 h.

### Effect of GroEL on the very fast phase of fluorescence change

One explanation for the increase observed in the apparent rate constant of the very fast phase of change in fluorescence with increasing GroEL concentration (Fig. 4a) is that it represents an increase in the rate constant of very fast folding as a consequence of GroEL binding rapidly to  $I_{E3}$ , with the GroEL-bound protein folding either at the same rate as free  $I_{E3}$  or at a faster rate than does free  $I_{E3}$ .<sup>32,33</sup> This explanation appears unlikely because the apparent rate constant increases linearly with increasing GroEL concentration and does not saturate at high GroEL concentrations. On the other hand, the relative amplitude of the very fast phase of fluorescence change reaches its maximum value when the ratio of GroEL concentration to total monellin concentration reaches 0.5:2. These results suggest that, in the presence of GroEL, the very fast phase of fluorescence change arises because of the rapid binding of refolding monellin to GroEL, which is accompanied by a change in monellin fluorescence. In this case, the linear increase observed in the apparent rate constant of the very fast phase of fluorescence change with increasing GroEL concentration reflects an increase in the apparent rate of the binding of GroEL to the initially formed heterogeneous intermediate  $I_E$ . The slope of the dependence of the apparent rate constant yields a value of  $\sim 10^8 \text{ M}^{-1} \text{ s}^{-1}$  for the bimolecular rate constant of association of  $I_E$  with GroEL. Similar values have been obtained for the rate constant of binding of the partially structured forms of other proteins to GroEL.<sup>16,59,60</sup>

The observation that the relative amplitude of the very fast phase has reached a saturating value at a GroEL concentration at which the other phases of folding are still decreasing in amplitude (see the text below) indicates that the increase in the former is not due to a decrease in the latter. The relative amplitude of the very fast phase of fluorescence change increases with increasing GroEL concentration because the fluorescence of the  $I_E \cdot G$  complex is higher than that of  $I_E$  alone. The observation that it saturates at a concentration of GroEL at which the other phases are still decreasing indicates that, at present, it is not known whether the enhancement in the fluorescence of  $I_E$  upon binding GroEL is the consequence of an additional structure being induced in  $I_E$  by the binding event. For several other proteins, too, the binding of GroEL to partially structured forms leads to an enhancement of the fluorescence of the bound intermediate.<sup>12–15,17–21</sup> The observation that the very fast, fast, and slow phases of folding are all modulated in the presence of GroEL (Fig. 4) suggests that all three components of  $I_E$  ( $I_{E1}$ ,  $I_{E2}$ , and  $I_{E3}$ ) bind to GroEL during folding. It should be noted, however, that the data in Fig. 4a and b do not indicate whether the binding of each

component of  $I_E$  to GroEL is accompanied by an increase in fluorescence. It is possible, for example, that only the binding of  $I_{E1}$  and  $I_{E2}$  to GroEL leads to the observed increase in fluorescence upon binding, while the binding of  $I_{E3}$  to GroEL is not accompanied by any increase in fluorescence.

The observation that the relative amplitude of the very fast phase saturates at 0.5  $\mu\text{M}$  GroEL and does not increase upon a further increase in GroEL concentration suggests that this concentration of GroEL is sufficient for binding to 2  $\mu\text{M}$  refolding monellin. Since it is not known whether the fluorescence of all three components of  $I_E$  ( $I_{E1}$ ,  $I_{E2}$ , and  $I_{E3}$ ) is enhanced, it becomes difficult to determine the number of sites on GroEL to which the different components can bind, and whether they all bind to the same sites. It can only be said that each molecule of GroEL has four or fewer sites to which refolding monellin molecules can bind. It is evident, however, that the components of  $I_E$  whose fluorescence is enhanced as a consequence of binding must bind GroEL very tightly: the relative amplitude of the very fast phase of fluorescence change reaches its maximum value very abruptly, and not gradually, at 0.5  $\mu\text{M}$  GroEL.

It should be remembered that, in the absence of GroEL, the very fast phase of fluorescence change reflects the folding of  $I_{E3}$  to  $I_{VF}$ . It is possible that this very fast folding reaction, like the fast and slow folding reactions (see the text below), also occurs in the presence of GroEL, but the effect of GroEL on the kinetics of the very fast folding reaction appears to be masked by the fluorescence change accompanying the binding of GroEL to  $I_E$ .

### Effect of GroEL on the fast and slow phases of folding

The decrease in the apparent rate constant and in the relative amplitude of the fast phase of fluorescence change observed during the folding of 2  $\mu\text{M}$  monellin with an increase in GroEL concentration to 0.6  $\mu\text{M}$ , after which the fast phase is no longer detected (Fig. 4c and d), can have two explanations: (1) GroEL binds rapidly to  $I_{E1}$  molecules, and GroEL-bound  $I_{E1}$  ( $I_{E1} \cdot G$ ) is incapable of folding further. With increasing GroEL concentration, the concentration of folding-competent  $I_{E1}$  (that which is free in solution) decreases (as it binds to GroEL), leading to a decrease in both the apparent rate constant and the relative amplitude of the fast phase of folding (Figs. 4c and d). (2) GroEL binds rapidly to  $I_{E1}$  molecules to form  $I_{E1} \cdot G$ , which folds further to  $I_F \cdot G$  ( $I_{F1} \cdot G + I_{F2} \cdot G$ ). The values of the forward and backward rate constants of the  $I_{E1} \cdot G \leftrightarrow I_{F1} \cdot G$  reaction are such that  $I_{F1} \cdot G$  is very marginally populated. The  $I_{E1} \cdot G \rightarrow I_{F2} \cdot G$  transition is either silent to fluorescence change, which is unlikely because it would mean that the fluorescence of  $I_{F2} \cdot G$  is less than that of  $I_{F2}$ , or its rate has slowed to become the same as that of the  $I_{F2} \cdot G \rightarrow N$  transition ( $0.002 \text{ s}^{-1}$ ). In this case, virtually all  $I_{E1} \cdot G$  molecules would fold further by the  $I_{E1} \cdot G \rightarrow I_{F2} \cdot G \rightarrow N$  route, where  $I_{F2} \cdot G$  is a high-energy intermediate that is not significantly populated and

whose fluorescence, like that of  $I_{F2}$ , is the same as that of N. This second explanation appears likely because the fraction of molecules that form  $I_{E1}$  and, hence, that would fold *via* the  $U_1 \rightarrow I_{E1} \rightarrow I_{E1} \cdot G \rightarrow I_{F2} \cdot G \rightarrow N$  route matches the fraction of molecules that are found to fold completely to N (50–60%) (Fig. 3a).

Since about 60% of refolding molecules (total concentration, 2  $\mu$ M) form  $I_{E1}$  in 0.5 M GdnHCl (Fig. 3), the concentration of  $I_{E1}$  would be  $\sim 1.2$   $\mu$ M. The binding of  $I_{E1}$  to GroEL appears to be very tight, with both the relative amplitude and the rate constant of the fast phase reaching their limiting values of zero abruptly at 0.6  $\mu$ M GroEL (Fig. 4b). Thus, it appears that one molecule of GroEL binds tightly to two molecules of  $I_{E1}$ . Although GroEL is capable of binding to substrate proteins in both folding chambers simultaneously,<sup>61,62</sup> it is not known, at the present time, whether the two  $I_{E1}$  molecules bind in the same folding chamber or in both folding chambers.

It is more difficult to understand fully how GroEL modulates the slow phase of folding because the slow phase has a small amplitude. But the decrease in the apparent rate constant and in the relative amplitude of the slow phase of fluorescence change observed during the refolding of 2  $\mu$ M monellin with an increase in GroEL concentration to 2  $\mu$ M, after which the slow phase is no longer observed, can be explained by the rapid binding of GroEL to  $I_{E2}$ , if the GroEL-bound  $I_{E2}$  is incapable of folding further.

### Effect of GroEL on the very slow phase of refolding

The observation that the reduced amplitude of the very slow phase of fluorescence change during folding increases from 0% in the absence of GroEL to a saturating value of 25% in the presence of 2  $\mu$ M

GroEL can have two explanations: (1) either one or all of the late intermediates  $I_{VF}$ ,  $I_{F1}$ ,  $I_{F2}$ , and  $I_S$ , which have native-protein-like fluorescence in the absence of GroEL, are less fluorescent when bound to GroEL; or (2) the late intermediates retain native-protein-like fluorescence even when bound to GroEL, but one or more of the bound late intermediates are destabilized sufficiently so as to not be populated. For example,  $I_{F2} \cdot G$  may be destabilized sufficiently so that it becomes a high-energy intermediate, but the transition state separating it from N is not destabilized. In that case, the overall rate constant for the  $I_{E1} \cdot G \rightarrow I_{F2} \cdot G \rightarrow N$  reaction would become the same as that of the  $I_{F2} \rightarrow N$  reaction ( $0.002$   $s^{-1}$ ), but a fluorescence change will accompany the very slow  $I_{E1} \cdot G \rightarrow I_{F2} \cdot G \rightarrow N$  reaction because  $I_{E1} \cdot G$  and N differ in fluorescence. It would not be surprising that the folding of  $I_{E1}$  to  $I_{F2}$  is slowed down when these intermediates are bound to GroEL because the transformation of  $I_{E1}$  into  $I_{F2}$  involves a significant conformational change. On the other hand, the folding of  $I_{F2}$  to N involves only a very local conformational change (proline isomerization)<sup>47</sup> whose rate might not depend on whether  $I_{F2}$  is bound to GroEL or not. Once folding to N has been completed, the bound native protein would dissociate rapidly from the GroEL.

### Mechanism of folding in the presence of GroEL

The observed effects of GroEL on the very fast, fast, slow, and very slow phases of fluorescence change during folding (see the text above) have been used to propose the following mechanism to account for the folding of 2  $\mu$ M monellin in the presence of 2  $\mu$ M GroEL. The mechanism depicted in Fig. 6b includes the rate constants observed for

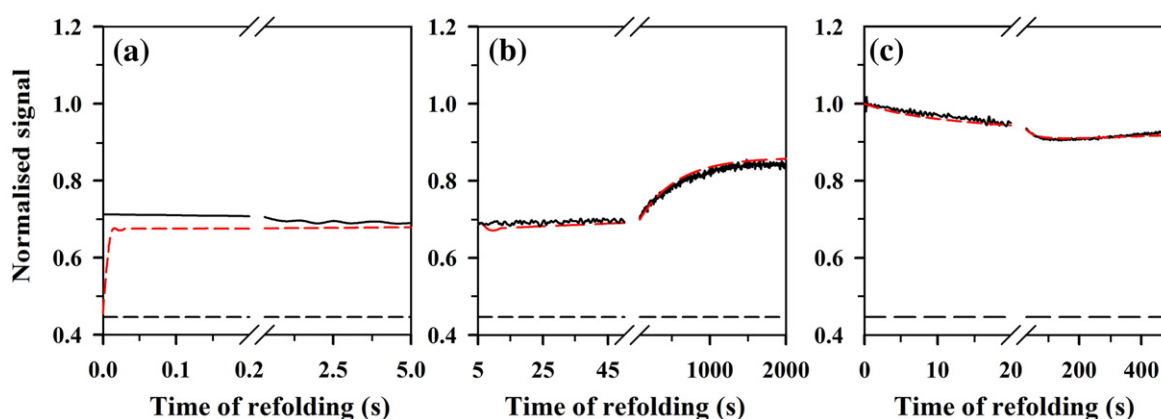


**Fig. 7.** Kinetic simulations using KINSIM<sup>65</sup> supporting the mechanism of refolding of monellin in the presence of GroEL. In each panel, the experimental data for the folding of 2  $\mu$ M monellin in the presence of 2  $\mu$ M GroEL (continuous black line) are shown along with the kinetic simulation (red broken line). The broken black line represents the signal of unfolded protein. (a and b) The refolding data and the simulation when folding is initiated in the presence of GroEL. (c) The refolding data and the simulation when GroEL is added 50 s after commencement of the refolding of monellin. The values of the rate constants used in the kinetic simulations are shown in the mechanism in Fig. 6b, as are the fluorescence values of the different states of the protein. For the simulation shown in (c), the fractions of U,  $I_{E1}$ ,  $I_{E2}$ ,  $I_{E3}$ ,  $I_{VF}$ ,  $I_{F1}$ ,  $I_{F2}$ ,  $I_S$ , and N present at 50 s of refolding were calculated from the values of the rate constants shown in the mechanism in Fig. 6a; the rate constants for the  $I_{E2} \cdot G \rightarrow I_S$ ,  $I_S \rightarrow I_{E2} \cdot G$ ,  $I_{E3} \cdot G \rightarrow I_{VF}$ , and  $I_{VF} \rightarrow I_{E3} \cdot G$  transitions were assumed to have values of  $0.1$   $s^{-1}$  (the same as that of  $I_{E2} \rightarrow I_S$ ; Fig. 6a),  $5$   $s^{-1}$  (Fig. 5a; see the text),  $7$   $s^{-1}$  (the same as that of  $I_{E3} \rightarrow I_{VF}$ ; Fig. 6a), and  $100$   $s^{-1}$ , respectively.

different transitions in the presence of GroEL (Figs. 4 and 5), as well as the rate constants observed for GroEL-independent steps, as shown in Fig. 6a. Also shown are the relative fluorescence values for different states describing the mechanism, as deduced from experimental data.

The mechanism is based on the following observations and assumptions: (1) GroEL (G) binds to all members of the  $I_E$  ensemble, with a bimolecular rate constant of  $10^8 \text{ s}^{-1}$  (Fig. 4a). Hence, the binding process in the presence of  $2 \mu\text{M}$  GroEL occurs with an apparent rate constant of  $200 \text{ s}^{-1}$ . (2) The fluorescence of  $I_{E1}$  and  $I_{E2}$  is enhanced (from 0.5 to 0.68 and 0.75, respectively), while that of  $I_{E3}$  remains unaltered, upon binding to GroEL. (3) All three binding steps are essentially irreversible because the binding is very tight. Based on the measured binding rate constant of  $10^8 \text{ s}^{-1}$  (Fig. 4a) and an arbitrarily chosen (for the simulation) dissociation rate constant of  $10^{-2} \text{ s}^{-1}$ , a value for  $K_d$  is obtained. GroEL has been reported to bind to folding intermediates of other proteins with similar affinity.<sup>59</sup> (4)  $I_{E2}\cdot\text{G}$  and  $I_{E3}\cdot\text{G}$  are incapable of folding further, while  $I_{E1}\cdot\text{G}$  can fold further to  $I_{F1}\cdot\text{G}$  and  $I_{F2}\cdot\text{G}$ . In previous studies, GroEL has been shown to bind very tightly in essentially an irreversible manner to the partially folded forms of other proteins.<sup>25,58,63,64</sup> (5) The fluorescence values of  $I_{F1}\cdot\text{G}$  and  $I_{F2}\cdot\text{G}$  are the same as those of free  $I_{F1}$  and  $I_{F2}$ , which are the same as that of N. (6) The  $I_{E1}\cdot\text{G} \rightarrow I_{F2}\cdot\text{G}$  step is essentially irreversible, with the backward unfolding step ( $I_{F2}\cdot\text{G} \rightarrow I_{E1}\cdot\text{G}$ ) being at least 20-fold slower than the forward step. (7) The rate constant of the  $I_{E1}\cdot\text{G} \rightarrow I_{F1}\cdot\text{G}$  step is assumed to be the same as that of the  $I_{E1}\cdot\text{G} \rightarrow I_{F2}\cdot\text{G}$  step and is at least as slow as the subsequent step. The rate constant for the unfolding of  $I_{F1}\cdot\text{G}$  is assumed to be the same as that for the unfolding of  $I_{F1}$  (Fig. 5a). This is 100-fold faster than that for its formation, thereby ensuring that the  $I_{E1}\cdot\text{G} \rightarrow I_{F2}\cdot\text{G} \rightarrow \text{N}$  pathway is effectively the only operational pathway for  $I_{E1}$  to fold. (8)  $I_{F1}\cdot\text{G}$  and  $I_{F2}\cdot\text{G}$  fold to N with the same rate constant as do free  $I_{F1}$  and  $I_{F2}$  (see the text above). (9) The fluorescence of GroEL does not change in the course of binding and folding monellin.

Figure 7 shows that a simulation of the folding of  $2 \mu\text{M}$  monellin in the presence of  $2 \mu\text{M}$  GroEL, according to the mechanism shown in Fig. 6b, with the rate constants for the various steps and with fluorescence values of the different intermediates as indicated, can adequately describe the folding process.

### GroEL unfolds refolding intermediates of monellin

The initial jump in fluorescence observed when GroEL is added at different times after the initiation of folding occurs for the same reason that an initial jump in fluorescence is observed when refolding is initiated in the presence of GroEL:  $I_{E1}$  and  $I_{E2}$  bind very rapidly to GroEL, with a consequent rise in their fluorescence. The observation that the initial jump in fluorescence, relative to the fluorescence of monellin folding in the absence of GroEL, is

observed even when GroEL is added at a time when the very fast and fast phases of folding are complete (so that  $I_{E1}$  and  $I_{E3}$  are no longer present) confirms that GroEL binds  $I_{E2}$  (Fig. 6b), which is the only one of the initially formed intermediates present at that long time.

The biphasic decrease in fluorescence, which follows the initial jump in fluorescence following delayed addition of GroEL (Fig. 5), appears to be the consequence of GroEL unfolding at least two intermediates that have formed prior to its addition. This conclusion is based on the observation that the time course of the change in the amplitude of the fast decrease in fluorescence parallels that of the change in the population of  $I_S$  during folding, while the time course of the change in amplitude of the slow decrease in fluorescence parallels that of the change in the populations of  $I_{F1}$  and/or  $I_{F2}$  during folding.

$I_S$  and  $I_F$  will unfold in the presence of GroEL if the chaperone binds more tightly to the intermediates ( $I_{E2}$  and  $I_{E1}$ , respectively) preceding them. In such a thermodynamic coupling mechanism, the energy of GroEL binding to the early intermediate is greater than the stability of the later intermediate, which leads to the unfolding of the later intermediate. Upon addition of GroEL, there will therefore be competition between the unfolding of the late intermediates ( $I_S$  and  $I_F$ ) and their further folding to N. The unfolding action of GroEL becomes apparent only because  $I_S$  and  $I_F$  fold to N at a very slow rate of  $\sim 0.002 \text{ s}^{-1}$ . This rate is much slower than the rates of unfolding of  $I_S$  ( $5 \text{ s}^{-1}$ ) and  $I_F$  ( $0.2 \text{ s}^{-1}$ ) observed in  $0.5 \text{ M}$  GdnHCl upon addition of GroEL (Fig. 5). The observation that  $I_S$  unfolds faster than  $I_F$  is in accordance with the prior observation that  $I_S$  is less stable than  $I_F$ .<sup>47</sup>

The maximum amplitude of the fast decrease in fluorescence upon addition of GroEL should occur when  $I_S$  is maximally populated, and the maximum amplitude of the slow decrease in fluorescence should correspond to the maximal population of  $I_F$ . The maximum observed reduced amplitudes of the two phases of fluorescence decrease are only 10% and 15% for the fast and slow phases, respectively.  $I_S$  and  $I_F$  are expected to be transiently populated to extents of 20–25% and 55–60%, respectively, during folding in the absence of GroEL.<sup>47</sup> There can be several explanations for the observed discrepancy between the expected maximum amplitudes of fluorescence decrease and the observed amplitudes upon delayed addition of GroEL: (1) the unfolding of  $I_S$  and  $I_F$  does not occur *via* a thermodynamic coupling mechanism as described above, but by GroEL binding to them preferentially and forcing them to unfold. Depending on the binding affinity of  $I_S$  and  $I_F$  for GroEL, only a fraction of these late intermediates would then unfold, resulting in a lower-than-expected accompanying decrease in fluorescence. This mechanism is unlikely because forced unfolding mechanisms proposed for GroEL involve conformational changes induced by the binding and hydrolysis of ATP,<sup>28,43,45</sup> which is not present in the

experiments described here. (2) Since GroEL binds tightly to the intermediates that precede  $I_S$  and  $I_F$  ( $I_{E2}$  and  $I_{E1}$ , respectively), and since GroEL-bound  $I_{E2}$  and  $I_{E1}$  have higher fluorescence than their unbound counterparts, the amplitudes of fluorescence decrease correspond to the difference in fluorescence between  $I_S$  and GroEL-bound  $I_{E2}$ , and between  $I_F$  and GroEL-bound  $I_{E1}$ . Moreover, the binding of GroEL to  $I_{E1}$  induces the unfolding of only  $I_{F1}$ , which is maximally populated to about 10%, and not  $I_{F2}$ , which is maximally populated to about 50%,<sup>47</sup> because  $I_{F2}\cdot G$  is much more stable than  $I_{F1}\cdot G$  (Fig. 6b). The kinetic simulation depicted in Fig. 7c indicates that this second mechanism can adequately explain the effect of the delayed addition of GroEL.

The final very slow increase in fluorescence, which follows the initial increase and then biphasic decrease in fluorescence upon delayed addition of GroEL, occurs with the same rate constant as that of the very slow phase of folding, which can be observed when folding is initiated in the presence of GroEL. It should therefore correspond to the very slow folding of late intermediates with GroEL bound (see the text above). The observation that this very slow increase in fluorescence is not observed when GroEL is added at times ( $>5$  s) after the very fast and fast phases of refolding had already been completed suggests that it does not have any contribution from the very slow folding of GroEL-bound  $I_S$ .

A major result of the present study is that the folding of monellin is effectively channeled along one of several different routes by GroEL. The chaperone plays, however, merely a passive role in which it acts by differentially binding to folding intermediates on the different folding pathways. Partially folded forms of proteins bind GroEL *via* exposed hydrophobic surfaces that are buried in binding-incompetent native forms of the proteins. The GroEL-bound forms of  $I_{E2}$  and  $I_{E3}$  presumably are incapable of folding further, while the GroEL-bound form of  $I_{E1}$  can fold further. It appears that  $I_{E2}$  and  $I_{E3}$  bind in such a manner that the subsequent folding reactions of  $I_{E2}\cdot G$  to  $I_S\cdot G$ , and of  $I_{E3}\cdot G$  to  $I_{VF}\cdot G$  are very slow compared to the unfolding reactions of  $I_S\cdot G$  and  $I_{VF}\cdot G$ , respectively. In contrast,  $I_{E1}$  binds GroEL in a manner that allows  $I_{E1}\cdot G$  to fold further. If  $I_{E2}$  and  $I_{E3}$  expose a greater hydrophobic surface to which GroEL can bind, then it might be the larger interaction interface that prevents  $I_{E2}\cdot G$  and  $I_{E3}\cdot G$  from folding further. This greater exposure of the hydrophobic surface is also likely to make  $I_{E2}$  and  $I_{E3}$  more aggregation-prone when GroEL is absent. Hence, by binding tightly to GroEL, refolding monellin would avoid utilizing aggregation-prone folding pathways. It is likely that ATP plays a role in the utilization of specific folding pathways when many pathways are available *via* modulation of the binding affinities of GroEL for the intermediates populating the different pathways.

A principal result of this study is the direct demonstration that GroEL can drive the unfolding

of partially folded intermediates populating the folding pathways.  $I_F$  and  $I_S$ , the two intermediates observed to unfold upon addition of GroEL, are not kinetically trapped or off-pathway intermediates but are instead productive (folding-competent) intermediates.<sup>47</sup> The unfolding appears to be purely the result of GroEL binding more tightly to the preceding intermediates  $I_{E1}$  and  $I_{E2}$ , than to  $I_F$  and  $I_S$ . Unfolding is enabled because the energies of binding of GroEL to  $I_{E1}$  and  $I_{E2}$  are greater than the stabilities of  $I_F$  and  $I_S$ .  $I_F$  is known to be more stable than  $I_S$  and  $I_{VF}$ ,<sup>47</sup> but the absolute stabilities of the late intermediates are not known. If GroEL binds to the early intermediates with a dissociation constant of 100 pM (see the text above), then in micromolar concentrations of GroEL, as used here and as found in the cell, the free energy of binding (the difference in the free energies of the free and bound GroEL =  $-RT\ln([GroEL]/K_d)$ ) would be  $-RT\ln(10^{-6}/10^{-10})$  or  $\sim 5.6$  kcal mol<sup>-1</sup>. Native monellin has a stability of 6.2 kcal mol<sup>-1</sup>; thus, thermodynamic coupling cannot cause it to unfold. But it appears that  $I_F$  and  $I_S$  have stabilities less than  $\sim 5.6$  kcal mol<sup>-1</sup>; thus, thermodynamic coupling does cause them to unfold. The result suggests that the ability of GroEL to bind to many different partially folded forms of proteins can sometimes lead to an undesired effect, namely, the unfolding of a productive folding intermediate.

## Materials and Methods

### Materials

All chemicals and reagents were obtained from Sigma-Aldrich (unless otherwise stated) and were of the highest purity grade. Double-distilled autoclaved water was used for all experiments.

### Purification of single-chain monellin

The purification protocol has been described previously.<sup>47</sup> The purity of the protein was checked with SDS-PAGE and was found to be  $>95\%$ . Electrospray ionization mass spectrometry indicated a pure protein with a mass of 11,403 Da. In addition, a second minor (10%) mass of 11,271 Da, which corresponds to the mass of the monellin sequence with the N-terminal methionine cleaved out, was observed. Typically, 100–250 mg of pure protein was obtained from 1 dm<sup>3</sup> of *E. coli* growth. In all studies, the monellin concentration was determined using the extinction coefficient  $\epsilon^{277\text{ nm}} = 1.46 \times 10^4 \text{ M}^{-1} \text{ cm}^{-1}$ .<sup>49</sup>

### Purification of GroEL

GroEL was purified from a GroE-overproducing strain of *E. coli* harboring the plasmid pOFX6.<sup>63,66</sup> Cells were grown overnight after induction with 0.05 mM isopropyl-D-1-thiogalactopyranoside. The purification protocol used has been described previously.<sup>33</sup> Very briefly, harvested cells were broken by sonication. This was followed by ion-exchange chromatography on a DE-52 column and then by hydrophobic interaction chromatography on a phenyl

Sepharose CL-6B column, after which the GroEL was >95% pure. To remove small tryptophan-containing contaminating peptides, an extra step involving reactive red 120 agarose (type 3000 CL) resin was added: the tryptophan fluorescence emission spectrum of the eluted protein was very similar to that of *N*-acetyl tyrosine amide. GroEL was checked for its ability to prevent aggregation of refolding rhodanase.<sup>33</sup> In all experiments, the concentrations of GroEL refer to that of the 14-mer and were determined using an extinction coefficient of  $\epsilon$  (0.1%, 1 cm)=0.2 at 280 nm.<sup>67</sup> GroEL was stored at  $-80^{\circ}\text{C}$  in 20 mM Tris (pH 7.5) and 5 mM  $\text{MgCl}_2$  with 10% glycerol. A PD-10 column was used to buffer exchange the GroEL into a refolding buffer immediately before use.

### Buffers and solutions

The native (refolding) buffer used for all equilibrium and kinetic experiments was composed of 50 mM sodium phosphate, 0.1 M KCl, 1 mM DTT, and 0.5 mM ethylenediaminetetraacetic acid (pH 7). The presence of DTT in all buffers ensured that the monellin molecules did not form dimers through intermolecular disulfides. The unfolding buffer was a native buffer containing 5 M GdnHCl (ultrapure; 99.9% from USB). The concentrations of stock solutions of GdnHCl were determined by measurement of the refractive index. All measurements were carried out at room temperature ( $25^{\circ}\text{C}$ ). All buffer solutions were passed through 0.22- $\mu\text{m}$  filters and degassed before use.

### Fluorescence spectra

Fluorescence spectra were collected on a Spex Fluoromax-3 spectrofluorimeter. The protein sample was excited at 280 nm, and emission spectra were collected from 300 to 400 nm, with a response time of 1 s, an excitation bandwidth of 0.3 nm, and an emission bandwidth of 5 nm, using a 0.2-cm pathlength cuvette. Each spectrum was recorded as the average of five fluorescence emission wavelength scans.

### Equilibrium unfolding experiments

Protein (8–10  $\mu\text{M}$ ) was incubated at different concentrations of GdnHCl ranging from 0 to 6 M for 6 h. Fluorescence signals at equilibrium were measured on the stopped-flow module (SFM-4; Biologic), with which the kinetic experiments were also performed. The protein sample was excited at 280 nm, and fluorescence emission was monitored using a 340-nm bandpass filter. For each sample, the signal was averaged for 120 s.

### Kinetic experiments

Rapid (milliseconds) mixing of solutions and observation of kinetic processes during the protein folding reactions were performed using a Biologic SFM-4 machine. The mixing dead time was about 1.8 ms, using a cuvette of 0.08 cm pathlength with flow rates of  $5\text{ mL s}^{-1}$ . Fluorescence was excited at 280 nm, and fluorescence emission was measured using a 340-nm bandpass filter. Data were acquired in three time domains on different channels, with different sampling times for each domain. For refolding experiments, monellin was first unfolded for 6 h in an unfolding buffer. Twenty microliters of 20  $\mu\text{M}$  equilibrium-unfolded monellin was diluted into 180  $\mu\text{L}$  of

premixed native buffer and GroEL-containing native buffer, so that the final GroEL concentration was within the range of 0–4  $\mu\text{M}$ , the final monellin concentration was 2  $\mu\text{M}$ , and the final GdnHCl concentration was 0.5 M.

For measurement of the very slow phase of refolding, a Fluoromax-3 spectrofluorimeter was used. Fifty microliters of equilibrium-unfolded protein was diluted into 450  $\mu\text{L}$  of premixed GroEL and native buffer, so that the final GroEL concentration was within the range of 0–4  $\mu\text{M}$ , the monellin concentration was 2  $\mu\text{M}$ , and the GdnHCl concentration was 0.5 M.

### Size-exclusion chromatography

Size-exclusion chromatography was carried out with an AKTA Basic-10 HPLC system using an analytical prepacked Superose-6 column with a bed volume of 24 mL and a separation range of 5–5000 kDa. Samples were injected into the column using a 200- $\mu\text{L}$  loop and run at a flow rate of  $0.5\text{ mL min}^{-1}$ . The elution profile was observed by measurement of absorbance at 280 nm.

### Fluorescence anisotropy experiments

The refolding of 2  $\mu\text{M}$  monellin was initiated in the presence of different concentrations of GroEL using a stopped-flow machine with a mixing dead time of 2 ms. Samples of refolding monellin were collected, and refolding was allowed to reach completion at 2000 s after mixing. Fluorescence anisotropy measurements were then carried out in a 1-cm cuvette using the MOS-450/AF-CD instrument (Biologic). Since GroEL does not contain tryptophan, and since monellin has one tryptophan residue, the samples were excited at 295 nm, exciting only tryptophan and not tyrosine. Hence, GroEL alone did not show any fluorescence signal. An additional 300-nm bandpass filter (Asahi) was placed in front of the cuvette to ensure that no stray light reached the sample. Fluorescence emission was measured using a 360-nm bandpass filter (Asahi). For each sample, anisotropy was averaged for 500 s.

### Determination of free (unbound) monellin by ultrafiltration

Five hundred microliters of the sample produced by a stopped-flow refolding experiment was added to a 100-kDa NMWL Centricon from Millipore and spun at 1000g until  $\sim 100\ \mu\text{L}$  of the sample had passed through the Centricon membrane. This was repeated four times. The sample that passed through the membrane was collected, and its fluorescence emission spectrum from 300 to 400 nm was measured using a Fluoromax-3 spectrofluorimeter. The fluorescence signal at 348 nm was normalized to that of a solution of 2  $\mu\text{M}$  monellin in a refolding buffer containing 0.5 M GdnHCl, which was ultrafiltered under identical conditions. For experiments in which ATP was used, ATP was removed using a High-trap desalting column (GE) before the measurement of fluorescence.

### Delayed addition of GroEL to refolding monellin

A Biologic SFM-4 mixing module was used to mix 30  $\mu\text{L}$  of 40  $\mu\text{M}$  equilibrium-unfolded protein in 5 M GdnHCl buffer with 270  $\mu\text{L}$  of native buffer, such that the final GdnHCl concentration was 0.5 M, and the monellin

concentration was 4  $\mu\text{M}$ . The refolding mixture was aged for different lengths of time in a delay loop of 190  $\mu\text{L}$  volume (the intermixer volume was 220  $\mu\text{L}$ ). After different refolding times (from 0 ms to 1 h), 100  $\mu\text{L}$  of the refolding protein in the delay loop was mixed with 100  $\mu\text{L}$  of 4  $\mu\text{M}$  GroEL in a native buffer containing 0.5 M GdnHCl, so that the final GdnHCl concentration remained 0.5 M, and the final monellin and GroEL concentrations were both 2  $\mu\text{M}$ . A dead time of 15.5 ms was obtained using a 0.15-cm cuvette and a flow rate of 2  $\text{mL s}^{-1}$ . The fluorescence of the solution subsequent to mixing was measured at 340 nm, with excitation at 280 nm.

## Acknowledgements

We thank the members of our laboratory for discussions and comments on the manuscript. This work was funded by the Tata Institute of Fundamental Research and by the Department of Science and Technology, Government of India. J. B. U. was the recipient of a J. C. Bose National Research Fellowship from the Government of India.

## References

- Bhutani, N. & Udgaonkar, J. B. (2002). Chaperonins as protein-folding machines. *Curr. Sci.* **83**, 1337–1351.
- Kerner, M. J., Naylor, D. J., Ishihama, Y., Maier, T., Chang, H. C., Stines, A. P. *et al.* (2005). Proteome-wide analysis of chaperonin-dependent protein folding in *Escherichia coli*. *Cell*, **122**, 209–220.
- Horwich, A. L., Farr, G. W. & Fenton, W. A. (2006). GroEL–GroES-mediated protein folding. *Chem. Rev.* **106**, 1917–1930.
- Lin, Z. & Rye, H. S. (2006). GroEL-mediated protein folding: making the impossible, possible. *Crit. Rev. Biochem. Mol. Biol.* **41**, 211–239.
- Horwich, A. L., Fenton, W. A., Chapman, E. & Farr, G. W. (2007). Two families of chaperonin: physiology and mechanism. *Annu. Rev. Cell Dev. Biol.* **23**, 115–145.
- Noivirt-Brik, O., Unger, R. & Horovitz, A. (2007). Low folding propensity and high translation efficiency distinguish *in vivo* substrates of GroEL from other *Escherichia coli* proteins. *Bioinformatics*, **23**, 3276–3279.
- Grallert, H. & Buchner, J. (1999). Analysis of GroE-assisted folding under nonpermissive conditions. *J. Biol. Chem.* **274**, 20171–20177.
- Martin, J. (2002). Requirement for GroEL/GroES-dependent protein folding under nonpermissive conditions of macromolecular crowding. *Biochemistry*, **41**, 5050–5055.
- Melkani, G. C., Zardeneta, G. & Mendoza, J. A. (2005). On the chaperonin activity of GroEL at heat-shock temperature. *Int. J. Biochem. Cell Biol.* **37**, 1375–1385.
- Stan, G., Brooks, B. R., Lorimer, G. H. & Thirumalai, D. (2006). Residues in substrate proteins that interact with GroEL in the capture process are buried in the native state. *Proc. Natl Acad. Sci. USA*, **103**, 4433–4438.
- Stan, G., Lorimer, G. H., Thirumalai, D. & Brooks, B. R. (2007). Coupling between allosteric transitions in GroEL and assisted folding of a substrate protein. *Proc. Natl Acad. Sci. USA*, **104**, 8803–8808.
- Clark, A. C. & Frieden, C. (1999). The chaperonin GroEL binds to late-folding non-native conformations present in native *Escherichia coli* and murine dihydrofolate reductases. *J. Mol. Biol.* **285**, 1777–1788.
- Aoki, K., Motojima, F., Taguchi, H., Yomo, T. & Yoshida, M. (2000). GroEL binds artificial proteins with random sequences. *J. Biol. Chem.* **275**, 13755–13758.
- Brinker, A., Pfeifer, G., Kerner, M. J., Naylor, D. J., Hartl, F. U. & Hayer-Hartl, M. (2001). Dual function of protein confinement in chaperonin-assisted protein folding. *Cell*, **107**, 223–233.
- Tang, Y. C., Chang, H. C., Roeben, A., Wischniewski, D., Wischniewski, N., Kerner, M. J. *et al.* (2006). Structural features of the GroEL–GroES nano-cage required for rapid folding of encapsulated protein. *Cell*, **125**, 194–903.
- Gray, T. E., Eder, J., Bycroft, M., Day, A. G. & Fersht, A. R. (1993). Refolding of barnase mutants and pro-barnase in the presence and absence of GroEL. *EMBO J.* **12**, 4145–4150.
- Bhutani, N. & Udgaonkar, J. B. (2001). GroEL channels the folding of thioredoxin along one kinetic route. *J. Mol. Biol.* **314**, 1167–1179.
- Landry, S. J., Jordan, R., McMacken, R. & Gierasch, L. M. (1992). Different conformations for the same polypeptide bound to chaperones DnaK and GroEL. *Nature*, **355**, 455–457.
- Martin, J., Langer, T., Boteva, R., Schramel, A., Horwich, A. L. & Hartl, F. U. (1991). Chaperonin-mediated protein folding at the surface of groEL through a ‘molten globule’-like intermediate. *Nature*, **352**, 36–42.
- Robinson, C. V., Gross, M., Eyles, S. J., Ewbank, J. J., Mayhew, M., Hartl, F. U. *et al.* (1994). Conformation of GroEL-bound alpha-lactalbumin probed by mass spectrometry. *Nature*, **372**, 646–651.
- Corrales, F. J. & Fersht, A. R. (1995). The folding of GroEL-bound barnase as a model for chaperonin-mediated protein folding. *Proc. Natl Acad. Sci. USA*, **92**, 5326–5330.
- Gervasoni, P., Staudenmann, W., James, P., Gehrig, P. & Pluckthun, A. (1996). Beta-lactamase binds to GroEL in a conformation highly protected against hydrogen/deuterium exchange. *Proc. Natl Acad. Sci. USA*, **93**, 12189–12194.
- Gervasoni, P. & Pluckthun, A. (1997). Folding intermediates of beta-lactamase recognized by GroEL. *FEBS Lett.* **401**, 138–142.
- Goldberg, M. S., Zhang, J., Sondek, S., Matthews, C. R., Fox, R. O. & Horwich, A. L. (1997). Native-like structure of a protein-folding intermediate bound to the chaperonin GroEL. *Proc. Natl Acad. Sci. USA*, **94**, 1080–1085.
- Clark, A. C. & Frieden, C. (1997). GroEL-mediated folding of structurally homologous dihydrofolate reductases. *J. Mol. Biol.* **268**, 512–525.
- Horst, R., Bertelsen, E. B., Fiaux, J., Wider, G., Horwich, A. L. & Wuthrich, K. (2005). Direct NMR observation of a substrate protein bound to the chaperonin GroEL. *Proc. Natl Acad. Sci. USA*, **102**, 12748–12753.
- Elad, N., Farr, G. W., Clare, D. K., Orlova, E. V., Horwich, A. L. & Saibil, H. R. (2007). Topologies of a substrate protein bound to the chaperonin GroEL. *Mol. Cell*, **26**, 415–426.
- Katsumata, K., Okazaki, A., Tsurupa, G. P. & Kuwajima, K. (1996). Dominant forces in the recognition of a transient folding intermediate of alpha-lactalbumin by GroEL. *J. Mol. Biol.* **264**, 643–649.

29. Coyle, J. E., Jaeger, J., Gross, M., Robinson, C. V. & Radford, S. E. (1997). Structural and mechanistic consequences of polypeptide binding by GroEL. *Fold. Des.* **2**, R93–R104.
30. Feltham, J. L. & Gierasch, L. M. (2000). GroEL–substrate interactions: molding the fold, or folding the mold? *Cell*, **100**, 193–196.
31. Thirumalai, D. & Lorimer, G. H. (2001). Chaperonin-mediated protein folding. *Annu. Rev. Biophys. Biomol. Struct.* **30**, 245–269.
32. Coyle, J. E., Texter, F. L., Ashcroft, A. E., Masselos, D., Robinson, C. V. & Radford, S. E. (1999). GroEL accelerates the refolding of hen lysozyme without changing its folding mechanism. *Nat. Struct. Biol.* **6**, 683–690.
33. Bhutani, N. & Udgaonkar, J. B. (2000). A thermodynamic coupling mechanism can explain the GroEL-mediated acceleration of the folding of barstar. *J. Mol. Biol.* **297**, 1037–1044.
34. Baumketner, A., Jewett, A. & Shea, J. E. (2003). Effects of confinement in chaperonin assisted protein folding: rate enhancement by decreasing the roughness of the folding energy landscape. *J. Mol. Biol.* **332**, 701–713.
35. Jewett, A. I., Baumketner, A. & Shea, J. E. (2004). Accelerated folding in the weak hydrophobic environment of a chaperonin cavity: creation of an alternate fast folding pathway. *Proc. Natl Acad. Sci. USA*, **101**, 13192–13197.
36. Itzhaki, L. S., Otzen, D. E. & Fersht, A. R. (1995). Nature and consequences of GroEL–protein interactions. *Biochemistry*, **34**, 14581–14587.
37. Zhou, H. X. & Dill, K. A. (2001). Stabilization of proteins in confined spaces. *Biochemistry*, **40**, 11289–11293.
38. Ellis, R. J. (2003). Protein folding: importance of the Anfinsen cage. *Curr. Biol.* **13**, R881–R883.
39. Zahn, R., Perrett, S. & Fersht, A. R. (1996). Conformational states bound by the molecular chaperones GroEL and secB: a hidden unfolding (annealing) activity. *J. Mol. Biol.* **261**, 43–61.
40. Walter, S., Lorimer, G. H. & Schmid, F. X. (1996). A thermodynamic coupling mechanism for GroEL-mediated unfolding. *Proc. Natl Acad. Sci. USA*, **93**, 9425–9430.
41. Zahn, R., Axmann, S. E., Rucknagel, K. P., Jaeger, E., Lamiet, A. A. & Pluckthun, A. (1994). Thermodynamic partitioning model for hydrophobic binding of polypeptides by GroEL: I. GroEL recognizes the signal sequences of beta-lactamase precursor. *J. Mol. Biol.* **242**, 150–164.
42. Lin, Z. & Rye, H. S. (2004). Expansion and compression of a protein folding intermediate by GroEL. *Mol. Cell*, **16**, 23–34.
43. Chen, J., Walter, S., Horwich, A. L. & Smith, D. L. (2001). Folding of malate dehydrogenase inside the GroEL–GroES cavity. *Nat. Struct. Biol.* **8**, 721–728.
44. van der Vaart, A., Ma, J. & Karplus, M. (2004). The unfolding action of GroEL on a protein substrate. *Biophys. J.* **87**, 562–573.
45. Lin, Z., Madan, D. & Rye, H. S. (2008). GroEL stimulates protein folding through forced unfolding. *Nat. Struct. Mol. Biol.* **15**, 303–311.
46. Kimura, T., Uzawa, T., Ishimori, K., Morishima, I., Takahashi, S., Konno, T. *et al.* (2005). Specific collapse followed by slow hydrogen-bond formation of beta-sheet in the folding of single-chain monellin. *Proc. Natl Acad. Sci. USA*, **102**, 2748–2753.
47. Patra, A. K. & Udgaonkar, J. B. (2007). Characterization of the folding and unfolding reactions of single-chain monellin: evidence for multiple intermediates and competing pathways. *Biochemistry*, **46**, 11727–11743.
48. Kimura, T., Maeda, A., Nishiguchi, S., Ishimori, K., Morishima, I., Konno, T. *et al.* (2008). Dehydration of main-chain amides in the final folding step of single-chain monellin revealed by time-resolved infrared spectroscopy. *Proc. Natl Acad. Sci. USA*, **105**, 13391–13396.
49. Morris, J. A., Martenson, R., Deibler, G. & Cagan, R. H. (1973). Characterization of monellin, a protein that tastes sweet. *J. Biol. Chem.* **248**, 534–539.
50. Kohmura, M., Nio, N. & Ariyoshi, Y. (1990). Complete amino acid sequence of the sweet protein monellin. *Agric. Biol. Chem.* **54**, 2219–2224.
51. Spadaccini, R., Crescenzi, O., Tancredi, T., De Casamassimi, N., Saviano, G., Scognamiglio, R. *et al.* (2001). Solution structure of a sweet protein: NMR study of MNEL, a single chain monellin. *J. Mol. Biol.* **305**, 505–514.
52. Xue, W. F., Carey, J. & Linse, S. (2004). Multi-method global analysis of thermodynamics and kinetics in reconstitution of monellin. *Proteins*, **57**, 586–595.
53. Konno, T., Murata, K. & Nagayama, K. (1999). Amyloid-like aggregates of a plant protein: a case of a sweet-tasting protein, monellin. *FEBS Lett.* **454**, 122–126.
54. Konno, T. (2001). Multistep nucleus formation and a separate subunit contribution of the amyloidogenesis of heat-denatured monellin. *Protein Sci.* **10**, 2093–2101.
55. Zheng, L. & Brennan, J. D. (1998). Measurement of intrinsic fluorescence to probe the conformational flexibility and thermodynamic stability of a single tryptophan protein entrapped in a sol–gel derived glass matrix. *Analyst*, **123**, 1735–1744.
56. Ranson, N. A., White, H. E. & Saibil, H. R. (1998). Chaperonins. *Biochem. J.* **333**, 233–242.
57. Ranson, N. A., Farr, G. W., Roseman, A. M., Gowen, B., Fenton, W. A., Horwich, A. L. & Saibil, H. R. (2001). ATP-bound states of GroEL captured by cryo-electron microscopy. *Cell*, **107**, 869–879.
58. Viitanen, P. V., Donaldson, G. K., Lorimer, G. H., Lubben, T. H. & Gatenby, A. A. (1991). Complex interactions between the chaperonin 60 molecular chaperone and dihydrofolate reductase. *Biochemistry*, **30**, 9716–9723.
59. Sparrer, H., Lilie, H. & Buchner, J. (1996). Dynamics of the GroEL–protein complex: effects of nucleotides and folding mutants. *J. Mol. Biol.* **258**, 74–87.
60. Perrett, S., Zahn, R., Stenberg, G. & Fersht, A. R. (1997). Importance of electrostatic interactions in the rapid binding of polypeptides to GroEL. *J. Mol. Biol.* **269**, 892–901.
61. Braig, K., Simon, M., Furuya, F., Hainfeld, J. F. & Horwich, A. L. (1993). A polypeptide bound by the chaperonin groEL is localized within a central cavity. *Proc. Natl Acad. Sci. USA*, **90**, 3978–3982.
62. Ishii, N., Taguchi, H., Sasabe, H. & Yoshida, M. (1994). Folding intermediate binds to the bottom of bullet-shaped holo-chaperonin and is readily accessible to antibody. *J. Mol. Biol.* **236**, 691–696.
63. Viitanen, P. V., Lubben, T. H., Reed, J., Goloubinoff, P., O’Keefe, D. P. & Lorimer, G. H. (1990). Chaperonin-facilitated refolding of ribulose biphosphate carboxylase and ATP hydrolysis by chaperonin 60 (groEL) are K<sup>+</sup> dependent. *Biochemistry*, **29**, 5665–5671.
64. Zahn, R., Spitzfaden, C., Ottiger, M., Wuthrich, K. & Pluckthun, A. (1994). Destabilization of the complete protein secondary structure on binding to the chaperone GroEL. *Nature*, **368**, 261–265.



- 
65. Barshop, B. A., Wrenn, R. F. & Frieden, C. (1983). Analysis of numerical methods for computer simulation of kinetic processes: development of KINSIM—a flexible, portable system. *Anal. Biochem.* **130**, 134–145.
66. Fayet, O., Louarn, J. M. & Georgopoulos, C. (1986). Suppression of the *Escherichia coli* dnaA46 mutation by amplification of the groES and groEL genes. *Mol. Gen. Genet.* **202**, 435–445.
67. Tsurupa, G. P., Ikura, T., Makio, T. & Kuwajima, K. (1998). Refolding kinetics of staphylococcal nuclease and its mutants in the presence of the chaperonin GroEL. *J. Mol. Biol.* **277**, 733–745.